Geoderma 447 (2024) 116928

Contents lists available at ScienceDirect

Geoderma

journal homepage: www.elsevier.com/locate/geoderma

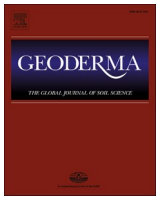

Assessing the 3D distribution of soil organic carbon by integrating predictions of water and tillage erosion into a digital soil mapping-approach: a case study for silt loam cropland (Belgium)

P. Baert [a,*], M. Vanmaercke [b], J. Meersmans [a]

[a] TERRA Teaching and Research Centre, Gembloux Agro-Bio Tech, University of Liège, Gembloux, 5030, Belgium
[b] Division of Geography and Tourism, Department of Earth and Environmental Sciences, University of Leuven, Heverlee, 3001, Belgium

ARTICLE INFO

Keywords:
Water erosion
Tillage erosion
Soil Organic Carbon
Digital Soil Mapping
WaTEM/SEDEM model

ABSTRACT

Although agricultural intensification has generally increased crop yields, it also resulted in a range of environmental issues. These include increased erosion rates and declined soil organic carbon (SOC) stocks. In order to improve our understanding on how erosion impacts the overall SOC storage capacity of croplands, this study analyses the 3D distribution of SOC as a function of water and tillage erosion in a conventionally ploughed field in the Belgian silt loam region. We present a novel methodological framework to integrate the output of an advanced erosion model as a co-variate within a Digital Soil Mapping (DSM) approach with the objective to create detailed SOC maps. More precisely, we combined (i) the Water and Tillage Erosion Model and Sediment Delivery Model (WaTEM/SEDEM), simulating spatial patterns of soil erosion and sediment deposition due to water and tillage erosions, with (ii) a SOC sampling campaign, resulting in a SOC spatial distribution model that considers both types of erosion. The results show that, as compared to plateaus, SOC stocks are nearly half as large along eroding slopes (i.e. convex slope positions affected by tillage erosion and steep slopes affected by water erosion). Yet, they are up to twice as large in areas characterized by sediment deposition (i.e. concave positions due to tillage erosion and foot slope positions due to water erosion). Our results further show that tillage erosion has a significant influence on the SOC stocks in the top 0.7 m and in particular on the top 0.4 m. The influence of water erosion is less strong but mostly significant along the entire depth profile. Overall, this work demonstrates the relevance of considering different erosion processes when aiming to predict spatial patterns of SOC. Considering the top 1 m and a WaTEM/SEDEM application at a resolution of 10 m our 3D SOC modelling approach obtained a coefficient of determination (R^2) of 0.62, a relative root mean square error (RRMSE) of 30.5 % and a relative mean absolute error (RMAE) of 26.0 %. While future work may likely lead to further improvements e.g. a more detailed SOC sampling network along the foot slopes and thalwegs in order to obtain a more spatially detailed prediction of the area characterized by depositions due to water erosion, we demonstrate the great potential of existing erosion and deposition models in doing so.

1. Introduction

Agricultural practices influence soil properties on both the short and long term (Larson and Pierce, 1994). Agricultural intensification has often boosted yields, but also resulted in many negative effects on soils. These include loss of biodiversity, increased susceptibility to erosion and decline in organic matter (Tilman et al., 2002). Chemical, physical and biological indicators such as texture, bulk density, pH, soil organic matter content and microbial biomass, are used typically to assess the health of agricultural soil (e.g. Li et al., 2023). As in many other regions worldwide, the progressive deterioration of the quality of agricultural soils has been identified as a severe threat across the Belgian loess belt (Goidts and van Wesemael, 2007). This while soils are considered a non-renewable resource on the scale of human generations (Lal, 2016). The growing awareness of the human impacts on soils has led researchers and decision-makers to develop tools to monitor soil quality, as well as policies to limit soil degradation by promoting sustainable practices (e.g. Borrelli et al., 2022).

Soil organic matter – and therefore soil organic carbon (SOC), which makes up roughly half of its mass – plays a fundamental role in the

* Corresponding author.
E-mail address: pierre.baert@uliege.be (P. Baert).

https://doi.org/10.1016/j.geoderma.2024.116928
Received 31 January 2024; Received in revised form 8 April 2024; Accepted 24 May 2024
Available online 7 June 2024

overall soil health status and the ecosystem services they support (Matson et al., 1997; Gardi et al., 2016). It is therefore a key property and measure of soil quality, associated with various physical, chemical and biological processes (Six et al., 2004). Meanwhile, organic matter undergoes a series of transformations as a result of biological activity as well as the physical and chemical conditions of the soil. These SOC dynamics are generally slow and changes are only detectable after several years to decades (Goidts and van Wesemael, 2007). In addition, SOC dynamics are by no means homogeneous (von Lützow et al., 2007). Rather, it consists of various carbon compounds with highly variable decomposition rates (Schmidt et al., 2011). Moreover, changes in land use and/or agricultural practices over long time periods of time (several decades to several centuries) are having a major impact on SOC evolution (Van Rompaey et al., 2002; van Wesemael et al., 2010). According to Meersmans et al. (2011) Belgian cropland soils lost around 8 % of its SOC stock between 1960′s and 2000′s. However, in the Belgian silt-loam region this loss appears to be bigger with values ranging between –22 % (Meersmans et al., 2009a) and –33 % (Goidts and van Wesemael, 2007) for the top 30 cm and an average decline of 20 % for the top 1.0 m (Meersmans et al., 2009a).

Soil erosion is the detachment and removal of soil material by a transporting agent. While it is largely a natural process depending on topography, weather and soil conditions, human activities can greatly influence this process by land cover changes and/or through land management practices (Borrelli et al., 2017). Historically, water erosion and wind erosion were considered as the main forms of soil erosion. However, over the last few decades, research and field data have shown that tillage erosion is another very important type of soil erosion in conventional agricultural systems (Govers et al., 1994). Finally, an important but relatively understudied form of anthropogenic erosion are soil losses due to crop harvesting root and tuber crops, which is typically uniform throughout the field (Kuhwald et al., 2022; Panagos et al., 2019). All these natural and anthropogenic forms of erosion affect soil properties and processes, and are widely recognized as a major cause of soil degradation in arable land, potentially leading to reductions in crop yields (Bakker et al., 2007; Wang et al., 2021). In the Belgium loess belt, the nation's most important food producing region, water and tillage erosions are more important than wind erosion (Poesen et al., 1996; Borrelli et al., 2022). Many studies identified muddy floods as one of the most threating hazards for local communities in this particular region (e.g. Evrard et al., 2007; Boardman and Vandaele, 2010; De Walque et al., 2017). Hence, limiting these types of erosions will be key in preserving the biodiversity and agronomic quality of these typically very fertile and high yielding soils.

Driven by the current-day threats of climate change and soil management impacts, numerous studies have been carried out to understand the evolution of soil carbon storage capacity and dynamics as a function of different factors and at different spatial and temporal scales. Many of these studies rely on the "scorpan" model (McBratney et al., 2003) with the objective to make spatially explicit predictions considering climate, land cover, soil properties and agro-management data, the so-called Digital Soil Mapping (DSM) approach. Nevertheless, great uncertainties remain about the exact impact of different types of erosion on the dynamics and spatial distribution of SOC; both in the plough layer and at greater soil depths within croplands (Goidts and van Wesemael, 2007). Similarly, we must stay cautious about generalizing these impacts on crop production to all agroecosystems (Bakker et al., 2007). Various models have been developed to predict the amount of SOC as a function of different soil-climate and soil-cover parameters, such as the best known "Rothamsted Carbon (ROTHC) model" or "DeNitrification-DeComposition (DNDC) model". Based on the carbon cycle, these models have been designed for a temporal analysis of SOC stocks, and therefore of soil carbon storage or loss, at different scales i.e. from plot level to national scale (Byrne and Kiely, 2009). However, these models come with shortcomings, as they do not take into account specific characteristics related to different landforms and/or associated erosion processes. As a consequence, in some cases these models will attribute a decrease in SOC due to soil erosion incorrectly to enhanced respiration rates (Chappell et al., 2015).

Another important shortcoming of these models is the poor characterization of the vertical heterogeneity of SOC along the soil profile. The empirical 3D SOC model of Meersmans (Meersmans et al., 2009b) this vertical heterogeneity of SOC up to 1 m depth predicts across Flanders (Belgium). It does so by taking into account soil type and land use factors, but ignores any potential topographically induced variability. Nonetheless, recent research has shown that the depth component is a critical dimension when considering the redistribution of SOC across erosional landscapes. For example, Doetterl et al. (2012) showed that the lateral transport of SOC due to erosion resulted in (i) a depletion of SOC topsoil across the entire depth profile at eroding sites along convex and steep slope positions and (ii) an accumulation of SOC, in particular at greater depths (below the plough layer), at deposition sites along concave and foot slope positions. Nonetheless, this study makes no differentiation in the type of erosion process. More recently, Borrelli et al. (2022) showed that the type of erosion varies greatly at local scales, highlighting the need to consider different types of erosion when studying the spatial distribution of SOC. Hence there exists an urgent need to develop a 3D SOC model that integrates the impact of different soil erosion processes on the vertical distribution across the entire profile. This implies the development of an improved sampling strategy (instead of classical approaches such as random, systematic, …) by taking into account the spatial distribution of different types of erosion using advanced models. This study therefore analyses the 3D distribution of SOC as a function of water erosion (E_w) and tillage erosion (E_t) in a conventionally cultivated field in the Belgian silt loam region. In doing so, we propose a novel methodological framework to integrate the output of an advanced erosion model (WaTEM/SEDEM) as a co-variate within a digital soil mapping (DSM) approach with the objective to create detailed SOC maps highlighting the erosion induced within-field redistribution of SOC.

2. Materials and methods

2.1. Study site description

The study was conducted on a single cropland field located in central Belgian loess region (i.e. in the commune of Orp-Jauche) at coordinates 50°42′26″N and 4°58′57″E and within an elevation range of 78 m to 99 m (Fig. 1). This field is characterized by an undulating topography and a temperate oceanic climate (Köppen classification Cfb) with an annual average rainfall amount of 758 mm, well distributed along the entire year, and an annual average temperature of 10,5 °C (IRM, 2023). As indicated on the European Soil Erosion Map croplands in the Belgian silt-loam region are characterized by fairly high soil loss rates even exceeding 5 ton ha^{-1} yr^{-1} (Borrelli et al., 2018). This field covers an area of 15.5 ha, is under cultivation since 1990 and is characterized by a 4-year crop rotation plan defined by a succession of *Solanum tuberosum*, *Triticum aestivum*, *Beta vulgaris,* vegetables – *Spinacia oleracea*, *Daucus carota, Allium cepa*. The field has a silt-loam texture with luvisols on the plateaus, cambisols along the slopes and colluvic regosols in the sediment deposition areas. Since 1990, no organic matter other than crop residues has been added to amend the soil.

The field is characterized by a typical convex-concave slope profile, exceeding 10 % at the most steep sections. It has two main thalwegs: one in the middle of the field and one along the Northwestern border. The latter thalweg has been ignored in this study because intensive activities with heavy machinery took place along the Northwestern border of the field. This displaced soil from the thalweg uphill, causing potentially significant disturbances of the soil profiles. Within the field there are no century-old charcoal production sites, which are common in the Belgian Loess region (e.g. Heidarian Dehkordi et al., 2020). In addition, the studied cropland has been conventionally ploughed using a classical

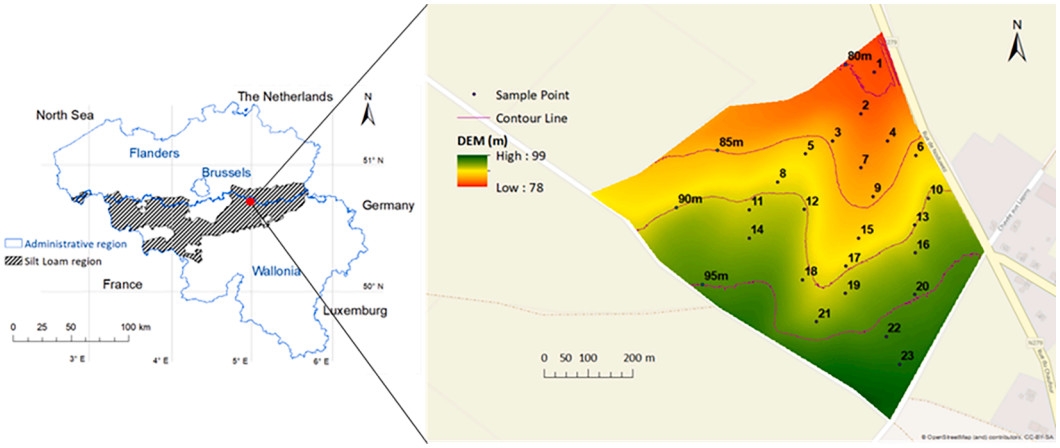

Fig. 1. Study site location within the Belgian silt loam region (red dot). DTM (1 m resolution) and contour lines of the field; 23 sample locations.

moldboard up to a depth of 30 cm for the last 50 years. Even though the region has known several historic land consolidations phases, our fields has been cultivated in a homogeneous and undivided manner for at least 30 years. Nevertheless, we avoided sampling along old field boundaries. For this, we consulted historic maps.

2.2. Methodological approach

The methodological flowchart displayed in Fig. 2 shows the approach used to achieve the objective of this study, i.e. assessing the 3D distribution of SOC as a function of water erosion (E_w) and tillage erosion (E_t) and to create a detailed SOC map. Firstly, the WaTEM/SEDEM model was run in the "default application mode", i.e. using a DEM with a resolution of 20 m (step 1). The resulting simulated patterns of E_w and E_t guided our sample design (step 2), where we identified 23 pixels showing a good range of E_w and E_t values as well as a wide spatial coverage within the studied cropland. Coordinates of the center of these pixels were used to collect soil samples at depths of 0.1 m to 1.0 m with an interval of 0.1 m (step 3). From the measured SOC contents of these samples, the corresponding SOC mass densities and SOC stock were calculated. Subsequently, a first order linear regression model was used to predict SOC stock as a function of depth, E_w and E_t (step 4). In addition, the WaTEM/SEDEM was applied in a "spatially refined mode", i.e. using a DEM with a resolution of 10 m (step 5) in order to find which resolution (10 m vs. 20 m) is most appropriate in a DSM context linking SOC spatial distribution to both E_w and E_t. Finally, the best model has been selected to create SOC maps considering a reference depth 0.3 m and 1.0 m (step 6).

2.3. Modelling water and tillage erosion with WaTEM/SEDEM

Typically, most process-based models predicting both water erosion and tillage erosion, such as SWAT, EPIC and LandSoil, require a large number of input parameters and variables (De Vente et al., 2013). However, the WaTEM/SEDEM model has generally acceptable input data requirements and has been successfully calibrated and validated in several regions, including the Belgian silt loam region at 20 m resolution (e.g. Verstraeten et al., 2002; Notebaert et al., 2006). This, in combination with the fact that it can simulate both water (i.e. sheet and rill) erosion, tillage erosion as well as sediment deposition, make it a widely applied model (Borrelli et al., 2021). Detailed descriptions of the model can be found in (Van Oost et al., 2000), (Van Rompaey et al., 2001), (Verstraeten et al., 2002).

Overall, WaTEM/SEDEM calculates the mean annual soil loss (A, (kg m^{-2} yr^{-1})) caused by water erosion in each pixel, based on the Revised Universal Soil Loss Equation (Eq. (1)):

$$A = R*K*L*S*C*P \quad (1)$$

where R is a rainfall erosivity factor (MJ mm h^{-1} m^{-2} y^{-1}); K is a soil erodibility factor (kg h MJ^{-1} mm^{-1}); L is a dimensionless slope length

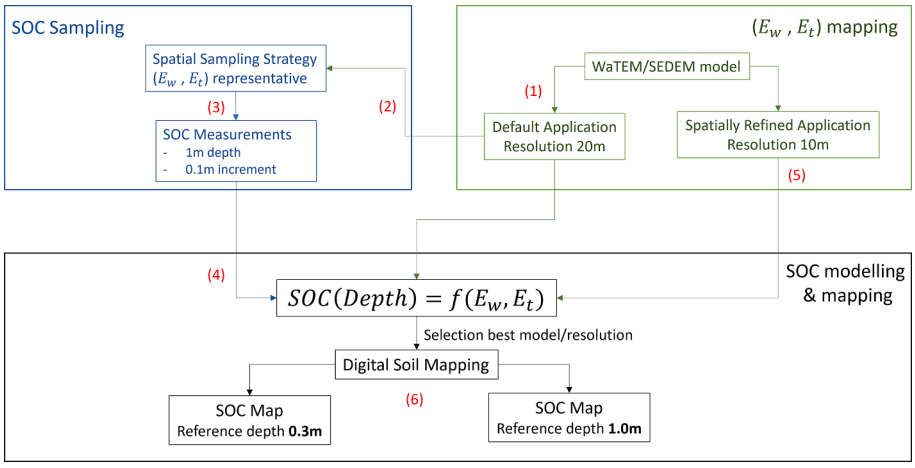

Fig. 2. Methodological flowchart illustrating the approach consisting of following steps: (1) Erosion mapping (E_w & E_t) with WaTEM/SEDEM at 20 m resolution ("default application"); (2) Sample strategy and design; (3) SOC measurements at depth of 0.1 m to 1.0 m with 0.1 m increment; (4) statistical model predicting SOC stock at different depths as a function of erosion (E_w & E_t); (5) mapping erosion (E_w & E_t) in a "spatially refined application" with WaTEM/SEDEM (10 m resolution); (6) Digital SOC stock mapping based on the best statistical model until reference depths of 0.3 m and 1.0 m.

factor; S is a dimensionless slope steepness factor; C is a dimensionless cropping and management factor, reflecting (amongst other things) the effect of vegetation cover and P is a dimensionless factor reflecting the effect of conservation practices.

The model also estimates an average sediment transport capacity for each pixel (T_c, (kg m^{-1})) using an empirical approach that relies on the assumption that T_c is proportional to the potential rill erosion (Eq. (2)) (van Oost et al., 2000). This rill erosion is the difference between total erosion and inter-rill erosion. The inter-rill erosion on each turn has been calculated following the method developed by McCool et al. (1987).

$$T_c = K_{tc}*R*K*(LS - 4.12*S^{0.8}) \quad (2)$$

where R, K, L and S are the same as in Eq. (1) and K_{tc} (m) is a calibrated transport capacity parameter that depends on the environmental setting and pixel resolution. Using a sediment routing algorithm, WaTEM/SEDEM then calculates the long-term average net erosion or deposition (E_w, (kg m^{-2} yr^{-1})) in each pixel, based on A and T_c. More specifically, model transfers an amount of sediments downslope equal to the minimum of either T_c or the sum of A and sediments already transferred from upslope pixels. If T_c is smaller than this sum, the remaining sediments are deposited within the pixel.

In addition, WaTEM/SEDEM calculates the amount of erosion/deposition in each cell due to tillage practices (Van Oost et al., 2006) (Eq. (3)):

$$E_t = -k_{till}*d^2h/dx^2 \text{ with } k_{till} = b*D*\rho_s \quad (3)$$

where k_{till} (kg m^{-1}) is the tillage transport coefficient function of soil bulk density ρ_s (kg m^{-3}) and tillage depth D (m) considered identical in the field, b is a constant, h (m) is the height of a given pixel of the hillslope and x (m) is the distance in horizontal direction. As such, tillage erosion/deposition rates mainly depend on the profile curvature of the hillslope, with convexities typically resulting in erosion and concavities in deposition.

Running the model hence requires the following input data: (i) a DEM and a parcel map with the same resolution, and (ii) values for R, K, C, P and K_{tc} and (iii) the tillage transport coefficient k_{till} and the soil bulk density. In our study, we used DEMs and parcel maps with a resolution of 20 m (default application) and 10 m (spatially refined application). Both DEMs are the result of a DEM originally created at a resolution of 1 m (Public services of Wallonia, 2015) which were resampled using the ARCGIS aggregate tool (mean approach). We considered the field to be hydrologically isolated, i.e. all flow accumulation is produced within the field with no influence from adjacent fields. The rainfall erosivity index (R) was set to 753 MJ mm $ha^{-1}h^{-1}$ yr^{-1}, based on a rain kinetic energy equation for central Belgium (Verstraeten et al., 2006). The soil erodibility index (K) was assumed to be 0.45 t h MJ^{-1} mm^{-1}, based on field experiments carried out on Belgian loam soils (Bollinne and Rosseau, 1978). The vegetation cover index (C) was set to 0.37, i.e. an annual average index for our type of cropland rotation within Belgian loess region (Notebaert et al., 2006). The tillage transport coefficient (k_{till} = 600 kg m^{-1}), the soil bulk density (i.e. 1350 kg m^{-3}) and the K_{tc} value (i.e. 250 m) were derived from Notebaert et al. (2003) and Verstraeten et al. (2003). We used the WaTEM/SEDEM version 2004 which has been calibrated across the Belgian Loess region, where also our study area is located, considering 21 catchments (Verstraeten and Poesen, 2001). More precisely, 5 out of 21 catchments used to calibrate this version of the model are located within a radius of 15 km from our study site. These 5 sites have similar land use (cropland dominated) and soil type (silt loam dominated) settings than our studied field. Also the L and S values were calculated within the model application, using the Nearing (1997) and McCool et al. (1987) approach.

2.4. Sampling strategy and techniques

In this study, the vertical heterogeneity of SOC was studied by taking soil cores until a depth of 1.0 m considering a sampling interval of 0.1 m. Using the output of the WaTEM/SEDEM default's setting at a resolution of 20 m, a total of 23 sample locations were selected following a model based sampling approach across the entire cropland (excluding the zone described in section 2.1) in a way that they had both a good spatial coverage (Fig. 1), as well as a large range of E_w and E_t values representative of the combined erosions distribution (Fig. 4C). As such, sampling locations occurred along the different topographical positions (i.e. plateau, convexity, steepest slope, concavity and thalweg). To reduce potential errors related to soil heterogeneity, three soil core replicates were taken at each of the 23 locations. These sampling points correspond to the vertices of an equilateral triangle, of which the base is perpendicular to an N-S axis and its center of gravity is located at the center of pixel of the WaTEM/SEDEM map at a resolution of 20 m (Fig. 3). The distance between this center of gravity and the sampling points is 0.5 m. In total, 690 soil samples were taken, across the 23 locations. Sampling was conducted on 16 and 23 March 2022, using a classical Edelman auger. Composites were formed from the three replicates (originating from the same location and depth increments), resulting in a total of 230 composite samples for which soil organic carbon (SOC) content (g C kg^{-1} soil) was analyzed. These analyses were conducted at the Provincial Centre for Agriculture and Rural Affairs laboratory in La Hulpe (Belgium) based on the dry combustion method and using an elemental analyzer (Primacs, Skalar Analytical, The Netherlands) according to the ISO 10694 norm.

2.5. SOC stock calculation and verification

SOC mass densities (kg C m^{-3}) are obtained by multiplying the SOC content (g C kg^{-1}) by the bulk density of the soil ρ_s (g cm^{-3}) (Eq. (4)). To obtain bulk density of all composite samples, a pedo-transfer function (Manrique and Jones, 1991) (Eq. (5)) was used. The SOC stock (kg C m^{-2}) of a layer is then calculated by multiplying the SOC mass density (kg C m^{-3}) by the thickness (m) of the corresponding layer (Eq. (6)). In our study, the thickness of this layer corresponds to the vertical sampling distance of 0.1 m. Subsequently, the SOC stock (kg C m^{-2}) for (i) the topsoil (i.e. until reference depth of 0.3 m), (ii) the total soil profile (until a reference depth of 1.0 m thickness), (iii) the intermediate soil layer (i.e. between 0.3 m and 0.5 m depth) and (iv) the subsoil (i.e. between 0.5 m and 1.0 m depth) were calculated by summing the SOC stock values of the corresponding layers of 0.1 m.

$$\text{SOC mass density} = \rho_s*\text{SOC content } *10^{-3} \quad (4)$$

$$\rho_s = 1.66 - 0.318*(\text{SOC content}*10^{-1})^{1/2} \quad (5)$$

$$(\text{SOC stock})_{layer} = (\text{SOC mass density})_{layer}*(\text{Thickness})_{layer} \quad (6)$$

The model of Meersmans et al., (2009b) (Eq. (7)) was applied to fit a depth distribution curve through the calculated SOC mass densities at

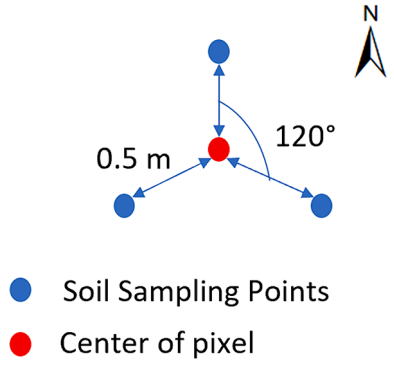

Fig. 3. Soil sampling points of a pixel.

each sample location:

$$\text{if } z \leq T_d : SOC(z) = SOC_{surf}$$

$$\text{if } z > T_d : SOC(z) = A * e^{\alpha z} + SOC_{inf} \quad (7)$$

where z is the soil depth (m), T_d is the tillage depth (m), SOC(z) is the SOC mass density (kg C m^{-3}) at depth z, SOC_{surf} is the SOC mass density (kg C m^{-3}) at the surface, SOC_{inf} is the SOC mass density (kg C/m^{-3}(−|-)) at the bottom of the soil profile and α is a constant which determines the shape of the exponential part of the curve.

2.6. Constructing a SOC map as a function of depth, E_w and e_t

SOC stocks for each soil depth as well as for the above described soil reference depths were predicted as a function E_w and E_t using a first order linear model (Eq. (8)).

$$SOC(d) = A_d + a_d * E_w + b_d * E_t \quad (8)$$

where SOC(d) is the SOC stock (kg C m^{-2}) at the depth d (m), E_w is the net amount water erosion/deposition (t ha^{-1} yr^{-1}), E_t is the tillage erosion (t ha^{-1} yr^{-1}) and A_d, a_d, b_d are fitted parameters.

After the calibration phase, during which the linear regression model parameters have been calculated, the model performance was assessed by calculating the coefficient of determination (R^2). Because of the small numbers of sample locations, the model was validated using the leave-one-out cross-validation (LOOCV). More precisely, the precision of the model has been calculated using the relative root mean square error (RRMSE) (%) (Eq. (9)), whereas its accuracy with the relative mean absolute error (RMAE) (%) (Eq. (10)). This model was then used to build a SOC stock map for the topsoil (until a depth of 0.3 m) and for the entire soil profile (until a depth of 1.0 m).

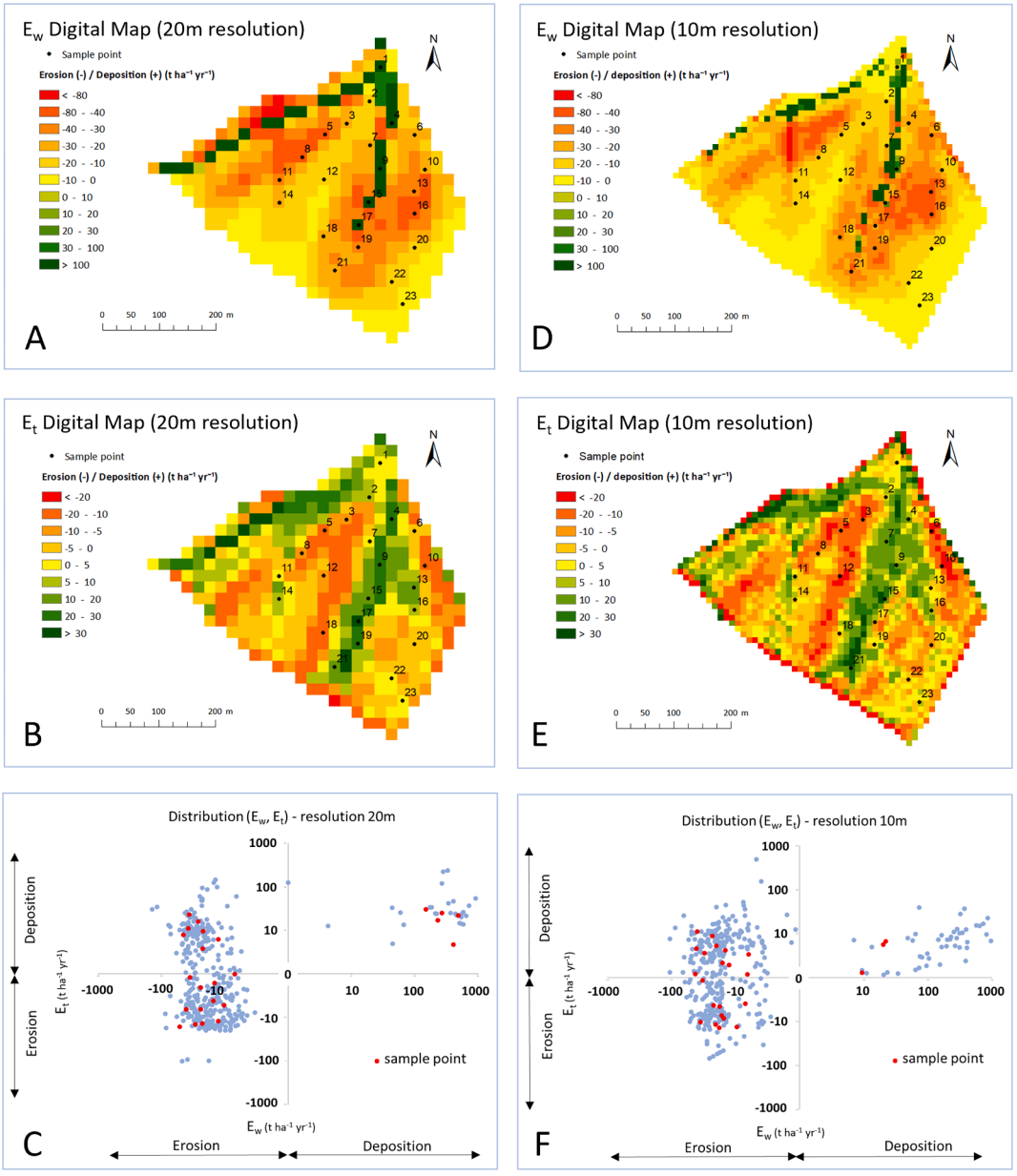

Fig. 4. Sample locations and WaTEM/SEDEM model output with (A) & (D) the water erosion (E_w) maps, (B) & (E) the tillage erosion (E_t) maps and (C) & (F) E_w, E_t prediction for all pixels (blue dots) and sample locations (red dots), considering the default (20 m, resolution) and the spatially refined (10 m, resolution) application modes, respectively.

$$\text{RRMSE} = \text{REQM}/(1/n^* \sum y_{obs})^*100 \quad \text{with REQM} = (\sum (y_{pred} - y_{obs})^2 / n)^{1/2} \tag{9}$$

$$\text{RMAE} = \text{MAE}/(1/n^* \sum y_{obs})^*100 \quad \text{with MAE} = \sum |y_{pred} - y_{obs}|/n \tag{10}$$

where y_{obs} is the observed value; y_{pred} is the value predicted by the model; and n is the number of samples.

2.7. Software

Modeling calculations were conducted in RStudio© software version 1.4.1717. E_w and E_t digital maps have been built with the WaTEM/SEDEM version 2014 for Windows©. All the maps were created with ESRI's ArcGIS© version 10.5.1 and use the "Belgian Lambert 2008" (EPSG:3812) geographic projection system.

3. Results and discussion

3.1. Water and tillage erosion mapping

Fig. 4A and 4B show respectively the simulated patterns of E_w and E_t at a 20 m resolution, using the WaTEM/SEDEM model. Both maps show clear contrasts in both the amount and spatial patterns of erosion and deposition. On the E_w map, 93 % of pixel showed net erosion and 7 % deposition. For the E_t map, 55 % showed erosion and 45 % deposition. Overall, the low number of deposition pixels in the E_w digital map relates to Eq. (2), which assumes that the transport coefficient T_c is proportional to the potential amount of rill erosion. As this potential is generally high, deposition only occurs at flatter hillslope bottoms. Yet, the amounts of deposition can be large in this area.

In the E_t, the field is topographically balanced, resulting in a comparable number of erosion and deposition pixels. E_t values range from -19 t ha^{-1} yr^{-1} (erosion) to 31 t ha^{-1} yr^{-1} (deposition) while E_w values vary from -69 t ha^{-1} yr^{-1} to 650 t ha^{-1} yr^{-1}. Fig. 4C presents a comparison of the E_w and E_t value of each pixel (Fig. 4C).

Fig. 4 further shows that applying WaTEM/SEDEM at a resolution of 20 m (Fig A & B) or at a resolution of 10 m (Fig. 4 C & D) results in overall similar spatial patterns. Nonetheless, E_w and E_t predictions can be fairly different for specific locations. This has consequences for the total sediment production, deposition and export, in that sense that these values are respectively 5.3 %, 4.3 % and 17.3 % lower at 10 m resolution as compared to the 20 m resolution (Table 1).

When looking to the erosion maps at 10 m resolution, we notice that for the E_w map 95 % of the pixels show erosion and 5 % deposition. For E_t, this is 52 % and 48 %. Comparing these maps with those obtained at 20 m resolution reveals that the area characterized by E_w deposition reduced *ceteris paribus* in the thalweg, whereas the E_t pixel values are even more balanced between erosion and deposition. Furthermore, one can notice a discontinuity in these E_w depositions along the thalweg axis, with some areas being characterized even by E_w erosion. In this particular topographical position is the slope steepness (S) rather low but the slope length (L) rather high, as such small variations in local slope steepness can result in contrasting predictions of erosion versus deposition. However, this may also indicate the need for further research in order to obtain a more detailed understanding as regards the sediment transport processes in this particular landscape unit, which may also be helpful to potentially improve the rooting function within the WaTEM/SEDEM deposition algorithm, including defining K_{tc} values.

Table 1
Total sediment production, deposition, export of the cultivated field from WaTEM/SEDEM model with two DEM resolution (10 m and 20 m).

	DEM Resolution	
	20 *m*	10 *m*
Total Sediment Production (t)	299	283
Total Sediment Deposition (t)	276	264
Total Sediment Export (t)	23	19

Fig. 4F shows the E_w versus E_t for each pixel, based on 10 m resolution applications (Fig. 4D, 4E). This graph shows some contrasts with the same comparison at 20 m resolution (Fig. 4E). The most remarkable differences can be found in the top right quadrant representing deposition in both E_w and E_t. By using the higher resolution DEM at 10 m, the number pixels characterized by deposition for both erosion processes clearly decreases. Deposition rates are typically an order of magnitude lower for the 10 m model run. This result indicates that the choice of the resolution has an important influence on the redistribution of the predicted E_w and E_t values across the sample locations, which has a particular strong impact in the depositional areas. Hence, increasing the number of samples in these depositional areas may be a good idea to reduce the associated source of uncertainty, and such, improve the present methodology in future research.

The WaTEM/SEDEM model was specifically developed in the early 2000 s to simulate the impact of soil conservation and sediment control measures as well as land use changes in the framework of an integrated catchment management, on the local soil loss and sediment delivery to rivers. Therefore, this model has been designed for large watersheds of hundreds to even thousands of hectares. The DEMS available at that time (i.e. early 2000 s), and the size of watersheds, justifies the default usage of the model at a resolution of 20 m resolution. However, the objective of our study was to use this model for a hydrologically isolated field of 15 ha in order to map E_w and E_t. As such, our results indicate clearly the limitations of using WaTEM/SEDEM in its default setting (20 m) when analyzing water and tillage erosion at the field-scale. Hence, further research is needed to develop a higher resolution version of the model with enhanced routing functions to better represent the sediment deposition process related to E_w. A first interesting attempt has been made by the development of SAGA WATEM at 5 m resolution (Oorts et al., 2019) but this model does not predict depositions and uses a general scaling factor of 1.4 on the LS-component of RUSLE applied on all pixels of the DEM in order to reduce the LS factor impact on water erosion. Also, additional studies are needed to improve sediment deposition mapping and values in slope concavities, outside the thalweg defined by the model. Finally, as our methodological approach involves the transformation of data between different GIS modelling-environments and associated raster formats (e.g. RST, GeoTIFF), we noticed a relatively small offset of the raster grid of ca. 3 m. This off-set is smaller than the resolutions of the SOC and erosion maps considered in this study (i.e. 20 m and 10 m), and as such, it most probably won't have any important influence on the final outcomes, but could still introduce a small source of error. Hence, in future research this could become an important issue to address, especially when carrying out this kind of DSM exercise considering a smaller resolution, for example at 5 m.

3.2. SOC measurements, calculation and verification

Fig. 5 shows the boxplots of the SOC stock values across all 23 sample locations for the topsoil (top 0.3 m), the entire profile (top 1.0 m), the subsoil (0.5 m − 1.0 m) and the intermediate soil layer (0.3 m − 0.5 m). The mean SOC stock for the entire profile (top 1.0 m) is 6.3 ± 0.5 kg C m^{-2} (Fig. 5), which is slightly lower than the average top 1.0 m SOC stock of 6.8 kg C m^{-2} as reported by Meersmans et al., (2009a) for well drained cropland soils across the Belgian silt-loam region corresponding in 2006. Roughly two third of this SOC is stored in the topsoil as indicated by the average SOC stock of 4.2 ± 0.2 kg C m^{-2} within the top 0.3 m. This value falls within the range of values reported by recent studies for Belgian silt loam cropland soils (i.e., 3.6 – 5.3 kg C m^{-2}; Sleutel et al., 2006; Goidts and van Wesemael, 2007; Meersmans et al., 2009a). As a consequence, the SOC stock in the intermediate soil layer (i.e. 1.1 ± 0.2

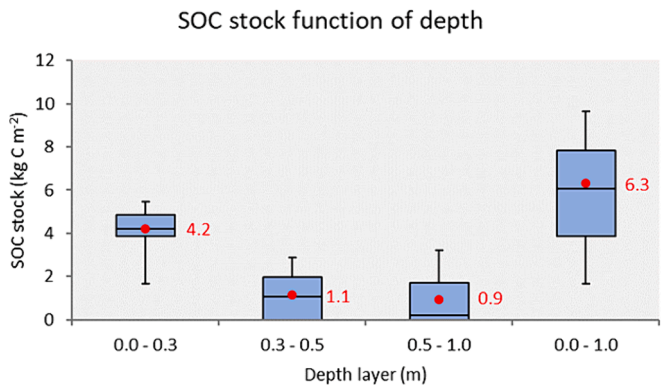

Fig. 5. Boxplot of SOC stock values considering all 23 sample locations for the topsoil (0.0 m – 0.3 m), intermediate soil layer (0.3 m – 0.5 m), subsoil (0.5 m –1.0 m) and entire profile (0.0 m – 1.0 m). Red dotes show mean values.

kg C m^{-2}) and the subsoil (0.9 kg ± 0.2 kg C m^{-2}) are fairly small. Moreover, the boxplot of the subsoil shows a skewed distribution with a median value of only 0.1 kg C m^{-2}. This can be attributed to the fact that in many sampling locations (and in particular at eroded sites) no SOC was detected at greater depths (below 0.5 m). SOC contents (Table A.1), SOC mass densities (Table A.2) and SOC stocks (Table A.3) values of all sample can be found in appendix A – supplementary tables.

The model of Meersmans et al., (2009b) describes the depth distribution of SOC in the plow layer as a constant and as exponentially declining below. When fitting this model through our SOC density measurements, an average tillage depth T_d of 0.23 ± 0.02 m was obtained. The mean SOC stock in the plow layer (i.e. 3.26 ± 0.32 kg m^{-2}) is similar to that of the top soil. The predicted values of the SOC distribution model (Eq. (7) were used to verify the overall trend in the depth distribution. An overview of the depth distributions of all 23 sample locations can be find in appendix B (Supplementary figures B1-B.23). To illustrate the impact of soil erosion on the SOC depth distribution of SOC, Fig. 6 displays 3 representative examples for (i) a highly eroded site (sample location 5), (ii) a depositional site (sample location 9) and a plateau site (sample location 23). In general, the eroded site has somewhat lower SOC mass densities near the surface (i.e. 12.1 kg C m^{-3} versus 14.2 kg C m^{-3} and 16.5 kg C m^{-3} for respectively the erosional, plateau and depositional site). However, most remarkable is the steep decline of SOC below the plough layer, with almost negligible SOC densities from 0.4 m onwards at the erosional site. At the two other sites (plateau and depositional) this decline with depth is more gradual. This is particularly true for the depositional sites, with SOC density values still ranging between 3 and 5 kg C m^{-3} near the bottom of the profile. As a result, the SOC stocks of the entire profile (i.e. top 1.0 m) at the erosional site (3.8 kg C m^{-2}) is only nearly half of that at the plateau site (6.4 kg C m^{-2}) and around 3 times smaller than that at the deposition site (10.8 kg C m^{-2}). The most likely explanation is that a large quantity of the SOC lost at the erosional sites was transported and buried at the depositional sites. This remarkable spatial variability of SOC stocks and associated depth distributions within fields highlights the caution that needs to be given when aiming to quantify SOC at larger scales (e.g. DSM

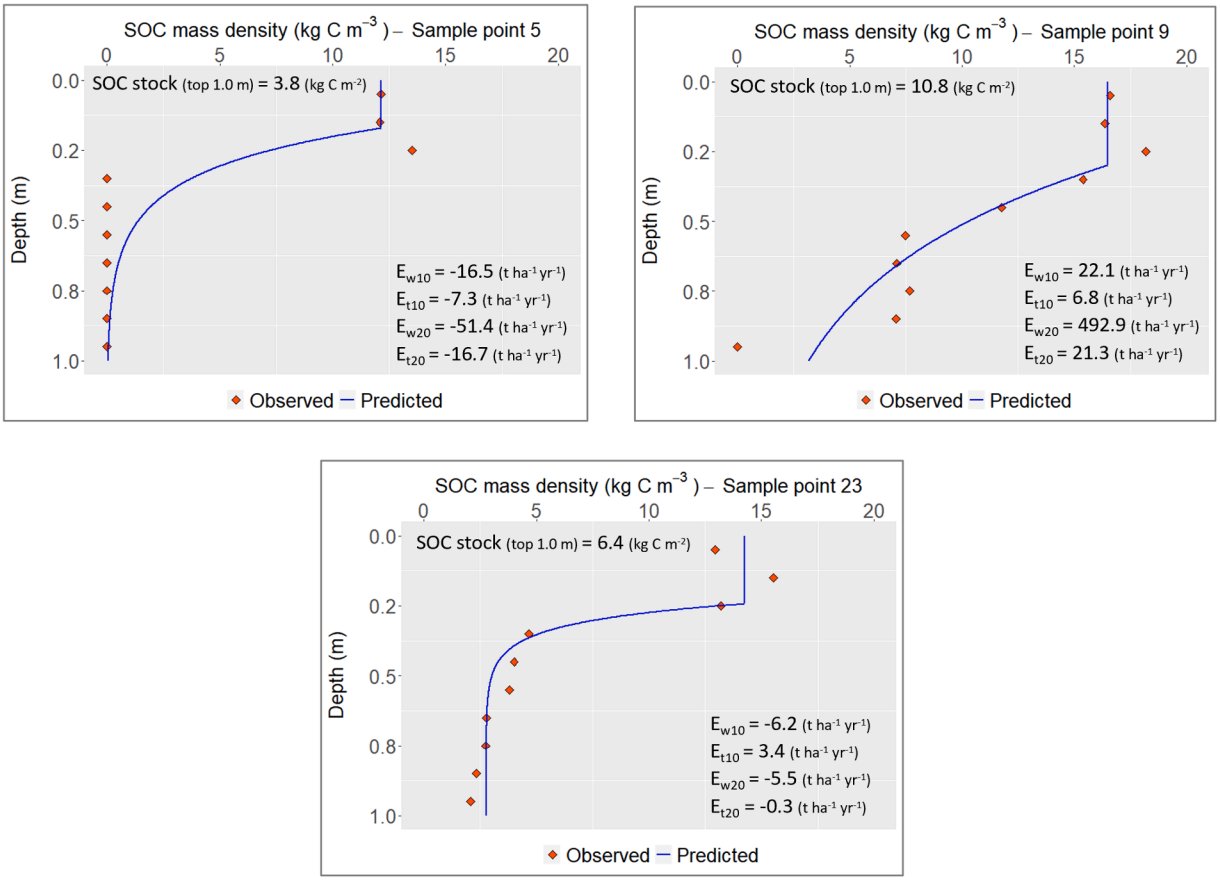

Fig. 6. SOC mass density depth distribution for a highly eroded site (sample location 5), a depositional site (sample location 9) and a plateau site (sample location 23). Red dots represent the SOC mass density value obtained from composite samples (originating from 3 replicates). The blue line represents the trend curve fitted after applying the model of Meersmans et al., (2009b). Top 1 m SOC stock, as well as water and tillage erosion values (at 20 m and 10 m resolutions) predictions as obtained from the WaTEM/SEDEM model (cf. Fig. 4), are given for each sample location. An overview of all sample locations can be found in appendix B – supplementary figures B.1 to B.23.

studies mapping SOC at the regional / national level). This because it often involves the risk of missing out on this erosion-induced SOC variability, and the resulting large SOC heterogeneity that may occur across agricultural landscapes.

3.3. SOC modelling as a function of erosion

Based on the erosion predictions using the 20 m DEM (i.e. the 'default' WaTEM/SEDEM application) the linear regression model, which expresses SOC stock at a given depth as a function of E_w and E_t, did not result in any statistically significant fit for the first 0.6 m (Table 2). However, this relationship was significant for E_w at a depth between 0.6 m and 1.0 m, whereas this was not the case for E_t. The corresponding R^2 values ranged between 0.11 and 0.52, while for the validation, we obtained RRMSE values in the range of 17.7 % to 272.0 % and RMAE values in the range of 14.7 % to 172.0 %. Furthermore, when considering the top, intermediate and subsoil layers, only in the subsoil (0.5 m − 1.0 m) and entire soil profile (0.0 m – 1.0 m) the SOC stocks are significantly modeled as a function of E_w, resulting in R^2 values of 0.42 and 0.34, RRMSE values of 128.9 % and 41.1 % and RMAE values of 106.3 % and 34.2 %, respectively.

Results further improve when considering the spatially refined application of the WaTEM/SEDEM model (i.e. at 10 m resolution). One can observe many more statistically significant relationships between SOC stock and both E_w and E_t at all depths (Table 2). The role of E_t seems to be particularly important for explaining SOC variations in the top 0.4 m of the soil profile ($p < 0.001$), but seems insignificant below 0.7 m. Meanwhile, the effect of E_w on SOC stocks seems smaller in this top layer. However, E_w remains an important variable for explaining SOC at greater depths. Overall, our model performance using erosion estimates at 10 m resolution are statistically better than when using estimates at 20 m resolution. This is particularly true for the upper part of the soil profile (0.0 m — 0.4 m) with R^2 values of around 0.6. At greater depths, performances diminish in terms of R^2, RRMSE and RMAE which can be partly explained by the fact that we have rather high variability and very low SOC values. Note that all model coefficients (for both E_t and E_w) are positive, indicating that SOC increases with increasing E_w and E_t values, or in other words predicting higher SOC stocks in depositional than erosional sites.

Concerning the SOC stock in topsoil (0.0 m − 0.3 m), intermediate soil (0.3 m − 0.5 m), subsoil (0.5 m − 1.0 m) and total soil (0.0 m − 1.0 m), the model output shows that E_w and E_t are significant variables, except for E_t in the subsoil. The topsoil (0.0 m – 0.3 m) and total soil (0.0 m – 1.0 m) seems to have good model performance values, i.e. R^2 values of 0.68 and 0.62, RRMSE of 15.0 % and 30.5 % and RMAE of 12.7 % and 26.0 % respectively, which is remarkably better than the results obtained when using the model's default setting.

Overall, our results indicate that the present approach is less suitable for predicting SOC per 0,1 m depth increment (especially at greater depth), but is particularly interesting for modelling SOC until a fixed reference depth, e.g. top 0.3 m and 1.0 m. Nevertheless our results also indicate that (i) E_t is for most affecting SOC in the upper 0.5 m of the profile, which can be explained by the fact that the considered cropland has been tilled until a depth of 30 cm, whereas (ii) E_w tends to have also an impact on SOC at greater depths (below 0.5 m of depth), which could be the consequence of a SOC stabilization mechanism in the buried sediments following the process of re-aggregation within zones characterized by significant E_w deposition (Doetterl et al., 2016).

3.4. SOC mapping

Given their good performance (Table 2), the topsoil and the entire profile models at 10 m resolution were used in combination with the corresponding E_w and E_t maps to create DSM SOC maps for the topsoil (0.0 – 0.30 m) and the entire profile (0.0 – 1.0 m) (Figs. 7, 8). Comparisons of these DSM SOC maps (Fig. 7) with the two erosion maps (Fig. 4) highlight the influence of both water and tillage erosion on the spatial distribution of SOC, with low SOC stocks occurring mainly in strongly eroded areas (e.g. convexity and steep slopes) and high stocks occurring along deposition areas (along the thalweg and, to a lesser extent, in the slope concavities). When considering the topsoil SOC map, the influence of E_w is in particular strong with high SOC values located along the thalwegs (Fig. 4F) in areas where predicted E_w indicate depositional values which are typically an order of magnitude bigger than elsewhere.

Overall, our topsoil SOC map corresponds well our observations, with half of the samples showing a deviation above 10 % (Fig. 7A). For the entire profile, the deviations are somewhat larger, with 20 out of 23 sample locations exceeding this 10 % (Fig. 7B). Yet, these deviations appear to show no clear spatial pattern of these under / over estimation. These fairly good model performances are also confirmed by Fig. 8, showing a good agreement between observed and predicted SOC stock values for these 23 sample locations areas. Nonetheless, one can notice that under- or overestimations are somewhat linked to the SOC stock

Table 2
Performance of the linear model expressing SOC stock (kg C m^{-2}) as a function of water erosion (E_w) and tillage erosion (E_t) with the level of significance of the parameters of E_w and E_t variables (with. $p < 0.1$, * $p < 0.05$, ** $p < 0.01$ and *** $p < 0.001$), coefficient of determination (R^2) for the calibration, relative root mean square error (RRMSE) (%) and relative mean absolute error (RMAE) (%) for the validation. The upper part of the table considers SOC stocks for every 0.1 m depth increment along the entire profile. The lower part of the table presents SOC stocks from the topsoil (0.0 m – 0.3 m), intermediate layer (0.3 m − 0.5 m), the sub soil (0.5 m −1.0 m) and entire profile (0.0 m – 1.0 m).

	20 m resolution (default application)					10 m resolution (spatially refined application)				
	Calibration			LOOCV		Calibration			LOOCV	
Depth (m)	E_w	E_t	R^2	RRMSE (%)	RMAE (%)	E_w	E_t	R^2	RRMSE (%)	RMAE (%)
0.0 – 0.1		.	0.25	17.7	14.7	*	***	0.63	12.8	10.0
0.1 – 0.2			0.14	20.5	15.1	*	***	0.64	14.2	9.9
0.2 – 0.3			0.11	33.4	26.0	*	***	0.58	24.5	20.8
0.3 – 0.4			0.19	86.9	78.0		***	0.67	54.4	44.4
0.4 – 0.5	.		0.30	112.6	94.8	*	**	0.48	96.4	82.3
0.5 – 0.6			0.22	135.5	113.7		*	0.20	132.3	104.5
0.6 – 0.7	**		0.42	120.6	99.5	**	*	0.46	109.2	85.1
0.7 – 0.8	***		0.50	141.2	111.0	*		0.25	169.4	127.6
0.8 – 0.9	***		0.52	130.3	102.8	*		0.23	163.7	124.3
0.9 – 1.0	*		0.19	272.0	175.0			0.06	231.8	159.3
0.0 – 0.3			0.16	22.6	17.8	*	***	0.68	15.0	12.7
0.3 – 0.5	.		0.27	88.7	77.2	*	***	0.64	61.8	53.8
0.5 – 1.0	**		0.42	128.9	106.3	*		0.26	132.4	98.6
0.0 – 1.0	*		0.34	41.1	34.2	**	***	0.62	30.5	26.0

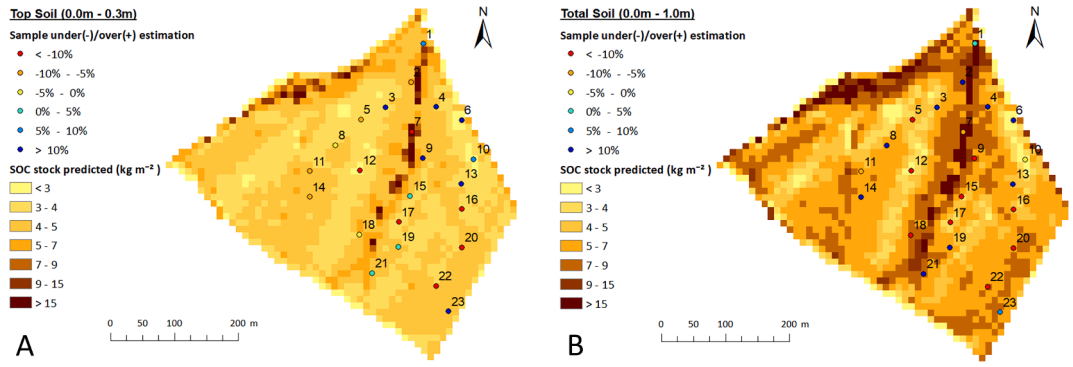

Fig. 7. Map of SOC stock value predictions (kg m^{-2}) in the (A) top soil (0.0 m – 0.3 m) and the (B) total soil profile (0.0 m – 1.0 m). The colored dots show the relative under- / overestimation at each sample location.

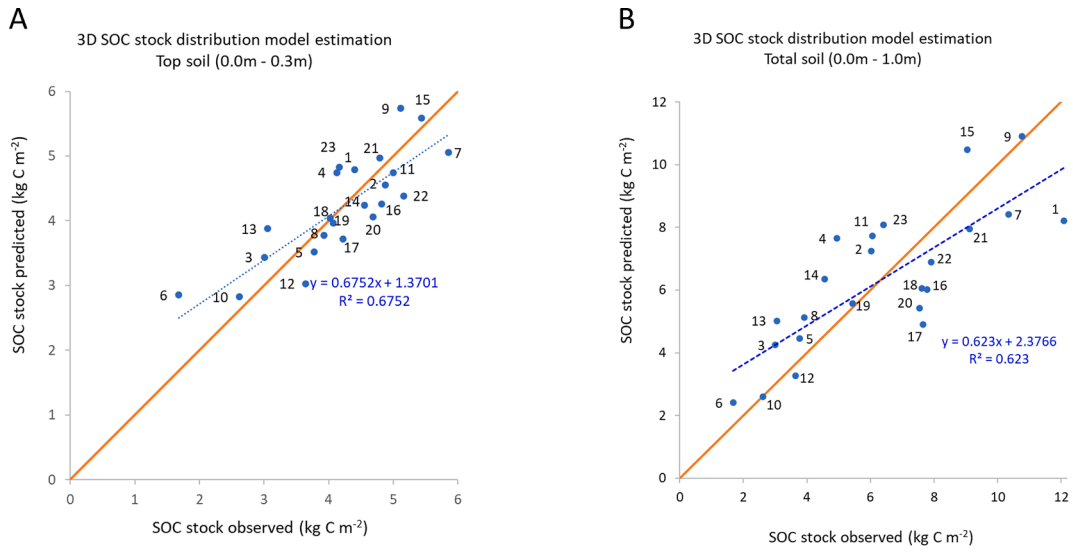

Fig. 8. Predicted versus observed SOC stock values (kg C m^{-2}) in (A) the top soil (0.0 m – 0.3 m) and (B) the total soil (0.0 m – 1.0 m); the 1:1 line is shown in orange; the linear regression line in dashed blue with its equation and R^2 value.

value. For the topsoil SOC map, slight overestimations mainly occur for lower observed SOC stock values (< 3 kg C m^{-2}) (Fig. 8A). For the total profile, values towards the higher SOC stock values (> 7kg C m^{-2}) tend to be underestimated, while samples characterized by a lower SOC stock tend to be overestimated (Fig. 8B). These results are in accordance with other empirical regression models which are optimized to correctly predict the mean but can't describe the full variability that occurs (e.g. Nearing, 1998). Although a LOOCV procedure has been applied, a future methodological improvement could be the application of a K-fold cross-validation procedure with a validation / calibration data split of 90 % – 10 % or 80 % – 20 % for instance. This was not possible in the present study due to the limited amount of sampling locations. Hence, increasing the number of sampling locations will be required. In that respect, it could be an option to avoid replicate sampling per sample location in order to maintain more or less the overall amount of samples while increasing the number of sampling locations.

3.5. *Limitations and future research perspectives*

Current-day large scale DSM studies aiming to quantify SOC stocks at catchment, regional or even larger scales often use covariate maps characterized by resolutions in the range of 100 m to 1 km. However, this study highlights the importance of within-field variability in SOC due to erosion. As such, we indicate the need to integrate high resolution (c. 10 m) E_w and E_t predictions in DSM-approaches in order to obtain reliable high-resolution SOC predictions, enabling a more robust assessment of the net impact of intensive conventional agricultural practices on SOC. We presented an innovative approach to better account for the impact of water and tillage erosion on SOC distribution. Nonetheless, some limitations can been highlighted which open interesting perspectives for future research:

- More samples in depositional landforms (i.e. concave and thalweg as typically being characterized by a large variation in E_w and E_t) should be taken to understand relationships between significant sediment deposition rates due to water erosion and associated SOC stock values and spatial distribution within these particular areas of the field.
- Find the right balance between number of replicates and number of sample locations to either (i) increase the number of observations enabling a robust modelling approach or (ii) make reliable within-location SOC measurements by increasing the number of replicates in the composite reducing the random error. By increasing the number of observations, we could also change our sampling strategy moving from a model based sampling approach to a design based sampling approach (e.g. random, systematic, …).
- Instead of using a model, integrate soil erosion measurements (either remote sensing based, e.g. lidar, or on-terrain using a proxy, e.g. ^{137}Cs) in the present approach in order to link directly erosion with SOC-value and its vertical distribution. This will be in particular

important in the E_w depositional areas where the WaTEM/SEDEM model seems to underperform by predicting in some pixels extreme high values and rather high variability along the thalweg-axe.
- Although WaTEM/SEDEM is most probably the best model predicting the spatial distribution of both long-term water and tillage erosion, improvements could still be considered with in particular improving (i) the DEM resolution and (ii) the water erosion deposition component, with a special focus on the routing function.
- Another soil erosion model than WaTEM/SEDEM may need to be considered when adopting the proposed DSM approach under specific conservation agriculture conditions such as no-till in which the contribution of E_t will be nihil.
- Enlarging the spatial extent of the sampling area considering multiple fields characterized by different topographic features and agricultural practices in order to apply the present approach within a first-order catchment (few 100s ha).
- Apply the present approach on the depth distribution model of Meersmans et al., (2009b) in order to model the associated parameter-values (i.e. SOC_{surf}, T_d, α, SOC_{inf}) as a function of E_w and E_t, and as such, obtain a full (non-linear) 3D model, rather than the usage of linear regression models per depth increments as being presented here.

4. Conclusion

We presented a novel approach to map the spatial distribution of SOC in relation to simulated patterns of water and tillage erosion and deposition. Our results highlighted the remarkably large impact of these erosion and deposition processes within a conventionally cultivated cropland. Water erosion had an effect on the entire profile while tillage erosion had mostly an impact on topsoil SOC. The SOC stocks are around 50 % lower on slopes subject to erosion than on plateaus and considerably higher in sediment deposition zones (along the thalweg and to a lesser extent in the slope concavity). Our results pave the way for further studies on other cropland with different pedological and topographical characteristics and agro-management practices; and more specifically, with a particular focus on the distribution of SOC within the sediment deposition zones. This reinforces the fact that additional cropland soil and erosion data are needed in order to build more advanced models that may allow the integration of water and tillage erosion predictions in DSM-approaches in order to obtain reliable high-resolution SOC predictions.

CRediT authorship contribution statement

P. Baert: Writing – original draft. **M. Vanmaercke:** Methodology, Software, Validation, Writing – original draft. **J. Meersmans:** Conceptualization, Methodology, Supervision, Validation, Writing – original draft, Writing – review & editing.

Declaration of competing interest

The authors declare that they have no known competing financial interests or personal relationships that could have appeared to influence the work reported in this paper.

Data availability

Data will be made available on request.

Acknowledgements

We're grateful to E. Vranckx for supporting this research by giving access to the studied field.

Appendix A. Supplementary data

Supplementary data to this article can be found online at https://doi.org/10.1016/j.geoderma.2024.116928.

References

Bakker, M.M., Govers, G., Jones, R.A., Rounsevell, M.D.A., 2007. The Effect of Soil Erosion on Europe's Crop Yields. Ecosystems 10, 1209–1219. https://doi.org/10.1007/s10021-007-9090-3.

Boardman, J., Vandaele, K., 2010. Soil erosion, muddy floods and the need for institutional memory. Area 42, 502–513. https://doi.org/10.1111/j.1475-4762.2010.00948.x.

Bollinne, A., Rosseau, P., 1978. L'érodibilité des sols de Moyenne et Haute Belgique. Utilisation d'une méthode de calcul du facteur K de l'équation universelle de perte de sol. Bull. Société Géographique Liège 127–140.

Borrelli, P., Robinson, D.A., Fleischer, L.R., Lugato, E., Ballabio, C., Alewell, C., Meusburger, K., Modugno, S., Schütt, B., Ferro, V., Bagarello, V., Oost, K.V., Montanarella, L., Panagos, P., 2017. An assessment of the global impact of 21st century land use change on soil erosion. Nat. Commun. 8, 2013. https://doi.org/10.1038/s41467-017-02142-7.

Borrelli, P., Van Oost, K., Meusburger, K., Alewell, C., Lugato, E., Panagos, P., 2018. A step towards a holistic assessment of soil degradation in Europe: Coupling on-site erosion with sediment transfer and carbon fluxes. Environ. Res. 161, 291–298. https://doi.org/10.1016/j.envres.2017.11.009.

Borrelli, P., Alewell, C., Alvarez, P., Anache, J.A.A., Baartman, J., Ballabio, C., Bezak, N., Biddoccu, M., Cerdà, A., Chalise, D., Chen, S., Chen, W., De Girolamo, A.M., Gessesse, G.D., Deumlich, D., Diodato, N., Efthimiou, N., Erpul, G., Fiener, P., Freppaz, M., Gentile, F., Gericke, A., Haregeweyn, N., Hu, B., Jeanneau, A., Kaffas, K., Kiani-Harchegani, M., Villuendas, I.L., Li, C., Lombardo, L., López-Vicente, M., Lucas-Borja, M.E., Märker, M., Matthews, F., Miao, C., Mikoš, M., Modugno, S., Möller, M., Naipal, V., Nearing, M., Owusu, S., Panday, D., Patault, E., Patriche, C.V., Poggio, L., Portes, R., Quijano, L., Rahdari, M.R., Renima, M., Ricci, G.F., Rodrigo-Comino, J., Saia, S., Samani, A.N., Schillaci, C., Syrris, V., Kim, H.S., Spinola, D.N., Oliveira, P.T., Teng, H., Thapa, R., Vantas, K., Vieira, D., Yang, J.E., Yin, S., Zema, D.A., Zhao, G., Panagos, P., 2021. Soil erosion modelling: A global review and statistical analysis. Sci. Total Environ. 780, 146494 https://doi.org/10.1016/j.scitotenv.2021.146494.

Borrelli, P., Panagos, P., Alewell, C., Ballabio, C., De Oliveira Fagundes, H., Haregeweyn, N., Lugato, E., Maerker, M., Poesen, J., Vanmaercke, M., Robinson, D. A., 2022. Policy implications of multiple concurrent soil erosion processes in European farmland. Nat. Sustain. 6, 103–112. https://doi.org/10.1038/s41893-022-00988-4.

Byrne, K., Kiely, G., 2009. Evaluation of Models (PaSim, RothC, CENTURY and DNDC) for Simulation of Grassland Carbon Cycling at Plot, Field and Regional Scale. EPA Grassl. Carbon Cycl. Rep. 20.

Chappell, A., Baldock, J., Sanderman, J., 2015. The global significance of omitting soil erosion from soil organic carbon cycling schemes. Nat. Clim Change Advance Online Publication. https://doi.org/10.1038/nclimate2829.

De Vente, J., Poesen, J., Verstraeten, G., Govers, G., Vanmaercke, M., Van Rompaey, A., Arabkhedri, M., Boix-Fayos, C., 2013. Predicting soil erosion and sediment yield at regional scales: Where do we stand? Earth-Sci. Rev. 127, 16–29. https://doi.org/10.1016/j.earscirev.2013.08.014.

De Walque, B., Degré, A., Maugnard, A., Bielders, C.L., 2017. Artificial surfaces characteristics and sediment connectivity explain muddy flood hazard in Wallonia. CATENA 158, 89–101. https://doi.org/10.1016/j.catena.2017.06.016.

Doetterl, S., Six, J., Van Wesemael, B., Van Oost, K., 2012. Carbon cycling in eroding landscapes: geomorphic controls on soil organic C pool composition and C stabilization. Glob. Change Biol. 18, 2218–2232. https://doi.org/10.1111/j.1365-2486.2012.02680.x.

Doetterl, S., Berhe, A.A., Nadeu, E., Wang, Z., Sommer, M., Fiener, P., 2016. Erosion, deposition and soil carbon: A review of process-level controls, experimental tools and models to address C cycling in dynamic landscapes. Earth-Sci. Rev. 154, 102–122. https://doi.org/10.1016/j.earscirev.2015.12.005.

Evrard, O., Bielders, C.L., Vandaele, K., Van Wesemael, B., 2007. Spatial and temporal variation of muddy floods in central Belgium, off-site impacts and potential control measures. CATENA 70, 443–454. https://doi.org/10.1016/j.catena.2006.11.011.

Gardi, C., Visioli, G., Conti, F.D., Scotti, M., Menta, C., Bodini, A., 2016. High Nature Value Farmland: Assessment of Soil Organic Carbon in Europe. Front. Environ. Sci. 4 https://doi.org/10.3389/fenvs.2016.00047.

Goidts, E., van Wesemael, B., 2007. Regional assessment of soil organic carbon changes under agriculture in Southern Belgium (1955–2005). Geoderma 141, 341–354. https://doi.org/10.1016/j.geoderma.2007.06.013.

Govers, G., Vandaele, K., Desmet, P., Poesen, J., Bunte, K., 1994. The role of tillage in soil redistribution on hillslopes. Eur. J. Soil Sci. 45, 469–478. https://doi.org/10.1111/j.1365-2389.1994.tb00532.x.

Heidarian Dehkordi, R., Denis, A., Fouche, J., Burgeon, V., Cornelis, J.T., Tychon, B., Placencia Gomez, E., Meersmans, J., 2020. Remotely-sensed assessment of the impact of century-old biochar on chicory crop growth using high-resolution UAV-based imagery. Int. J. Appl. Earth Obs. Geoinformation 91, 102147. https://doi.org/10.1016/j.jag.2020.102147.

IRM (2023). Climate statistics for the period 1991–2020, INS 25120 (Orp-Jauche; Belgique). Available at: https://www.meteo.be/fr/climat/climat-de-la-belgique/climat-dans-votre-commune.

Kuhwald, M., Busche, F., Saggau, P., Duttmann, R., 2022. Is soil loss due to crop harvesting the most disregarded soil erosion process? A review of harvest erosion. Soil Tillage Res. 215 https://doi.org/10.1016/j.still.2021.105213.
Lal, R., 2016. Soil health and carbon management. Food Energy Secur. 5, 212–222. https://doi.org/10.1002/fes3.96.
Larson, W.E., Pierce, F.J., 1994. The Dynamics of Soil Quality as a Measure of Sustainable Management, in: Defining Soil Quality for a Sustainable Environment. John Wiley & Sons, Ltd, pp. 37–51. https://doi.org/10.2136/sssaspecpub35.c3.
Li, X., Qiao, L., Huang, Y., Li, D., Xu, M., Ge, T., Meersmans, J., Zhang, W., 2023. Manuring improves soil health by sustaining multifunction at relatively high levels in subtropical area. Agric. Ecosyst. Environ. 353, 108539 https://doi.org/10.1016/j.agee.2023.108539.
Manrique, L.A., Jones, C.A., 1991. Bulk Density of Soils in Relation to Soil Physical and Chemical Properties. Soil Sci. Soc. Am. J. 55, 476–481. https://doi.org/10.2136/sssaj1991.03615995005500020030x.
Matson, P.A., Parton, W.J., Power, A.G., Swift, M.J., 1997. Agricultural Intensification and Ecosystem Properties. Science 277, 504–509. https://doi.org/10.1126/science.277.5325.504.
McBratney, A.B., Mendonça Santos, M.L., Minasny, B., 2003. On digital soil mapping. Geoderma 117, 3–52. https://doi.org/10.1016/S0016-7061(03)00223-4.
McCool, D.K., Brown, L.C., Foster, G.R., Mutchler, C.K., Meyer, L.D., 1987. Revised Slope Steepness Factor for the Universal Soil Loss Equation. Trans. ASAE 30, 1387–1396. https://doi.org/10.13031/2013.30576.
Meersmans, J., Van Wesemael, B., De Ridder, F., Fallas Dotti, M., De Baets, S., Van Molle, M., 2009a. Changes in organic carbon distribution with depth in agricultural soils in northern Belgium, 1960–2006. Glob. Change Biol. 15, 2739–2750. https://doi.org/10.1111/j.1365-2486.2009.01855.x.
Meersmans, J., van Wesemael, B., De Ridder, F., Van Molle, M., 2009b. Modelling the three-dimensional spatial distribution of soil organic carbon (SOC) at the regional scale (Flanders, Belgium). Geoderma 152, 43–52. https://doi.org/10.1016/j.geoderma.2009.05.015.
Meersmans, J., Van Wesemael, B., Goidts, E., Van Molle, M., De Baets, S., De Ridder, F., 2011. Spatial analysis of soil organic carbon evolution in Belgian croplands and grasslands, 1960-2006: SPATIAL ANALYSIS OF SOIL ORGANIC CARBON EVOLUTION. Glob. Change Biol. 17, 466–479. https://doi.org/10.1111/j.1365-2486.2010.02183.x.
Nearing, M., 1997. A Single, Continuous Function for Slope Steepness Influence on Soil Loss. Soil Sci. Soc. Am. J. 61 https://doi.org/10.2136/sssaj1997.03615995006100030029x.
Nearing, M.A., 1998. Why soil erosion models over-predict small soil losses and under-predict large soil losses. CATENA 32, 15–22. https://doi.org/10.1016/S0341-8162(97)00052-0.
Notebaert, B., Govers, G., Verstraeten, G., Oost, K.V., Poesen, J., Rompaey, A.V., 2003. Verfijnde erosiekaart Vlaanderen: eindrapport. Thema 220 Kwal. Bodem Erosie, MIRA-T 2003, Milieu en Natuurrapport Vlaanderen, thema's, Vlaamse Milieumaatschappij 345–355.
Notebaert, B., Vaes, B., Verstraeten, G., Govers, G., 2006. WaTEM/SEDEM version 2006 Manual.
Oorts, K., Buyle, S., Van de Wauw, J., 2019. Berekening van de potentiële erosiekaart per perceel in SAGA-GIS.
Panagos, P., Borrelli, P., Poesen, J., 2019. Soil loss due to crop harvesting in the European Union: A first estimation of an underrated geomorphic process. Sci. Total Environ. 664, 487–498. https://doi.org/10.1016/j.scitotenv.2019.02.009.
Poesen, J., Govers, G., Goosens, D., 1996. Verdichting en erosie van de bodem in Vlaanderen. Tijdschr. Van Belg. Ver. Voor Aardrijkskd. Stud, 141–181.
Public services of Wallonia, 2015. Relief de la Wallonie - Modèle Numérique de Terrain (MNT) 2013-2014 - Densité des mesures [WWW Document]. Wallonia Geoportal. URL https://geoportail.wallonie.be/catalogue/6029e738-f828-438b-b10a-85e67f77af92.html.
Schmidt, M.W.I., Torn, M.S., Abiven, S., Dittmar, T., Guggenberger, G., Janssens, I.A., Kleber, M., Kögel-Knabner, I., Lehmann, J., Manning, D.A.C., Nannipieri, P., Rasse, D.P., Weiner, S., Trumbore, S.E., 2011. Persistence of soil organic matter as an ecosystem property. Nature 478, 49–56. https://doi.org/10.1038/nature10386.
Six, J., Bossuyt, H., Degryze, S., Denef, K., 2004. A history of research on the link between (micro)aggregates, soil biota, and soil organic matter dynamics. Soil Tillage Res. 79, 7–31. https://doi.org/10.1016/j.still.2004.03.008.
Sleutel, S., De Neve, S., Singier, B., Hofman, G., 2006. Organic C levels in intensively managed arable soils – long-term regional trends and characterization of fractions. Soil Use Manag. 22, 188–196. https://doi.org/10.1111/j.1475-2743.2006.00019.x.
Tilman, D., Cassman, K.G., Matson, P.A., Naylor, R., Polasky, S., 2002. Agricultural sustainability and intensive production practices. Nature 418, 671–677. https://doi.org/10.1038/nature01014.
Van Oost, K., Govers, G., Desmet, P., 2000. Evaluating the effects of changes in landscape structure on soil erosion by water and tillage. Landsc. Ecol. 15, 579–591.
Van Oost, K., Govers, G., De Alba, S., Quine, T.A., 2006. Tillage erosion: a review of controlling factors and implications for soil quality. Prog. Phys. Geogr. Earth Environ. 30, 443–466. https://doi.org/10.1191/0309133306 pp487ra.
Van Rompaey, A., Govers, G., Puttemans, C., 2002. Modelling land use changes and their impact on soil erosion and sediment supply to rivers. Earth Surf. Process. Landf. 27, 481–494. https://doi.org/10.1002/esp.335.
Van Rompaey, A.J.J., Verstraeten, G., Van Oost, K., Govers, G., Poesen, J., 2001. Modelling mean annual sediment yield using a distributed approach. Earth Surf. Process. Landf. 26, 1221–1236. https://doi.org/10.1002/esp.275.
van Wesemael, B., Paustian, K., Meersmans, J., Goidts, E., Barancikova, G., Easter, M., 2010. Agricultural management explains historic changes in regional soil carbon stocks. Proc. Natl. Acad. Sci. u. s. a. 107, 14926–14930. https://doi.org/10.1073/pnas.1002592107.
Verstraeten, G., Van Rompaey, A., Poesen, J, Van Oost, K., Govers, G. & Stalpaert, L., 2003. Thema 2.20 Kwaliteit Bodem: erosie. In: MIRA-T 2003, Milieu en Natuurrapport Vlaanderen, thema's, Vlaamse Milieumaatschappij, 345-355.
Verstraeten, G., Poesen, J., 2001. Factors controlling sediment yield from small intensively cultivated catchments in a temperate humid climate. Geomorphology 40, 123–144. https://doi.org/10.1016/S0169-555X(01)00040-X.
Verstraeten, G., Van Oost, K., Van Rompaey, A., Poesen, J., Govers, G., 2002. Evaluating an integrated approach to catchment management to reduce soil loss and sediment pollution through modelling. Soil Use Manag. 18, 386–394. https://doi.org/10.1111/j.1475-2743.2002.tb00257.x.
Verstraeten, G., Poesen, J., Demarée, G., Salles, C., 2006. Long-term (105 years) variability in rain erosivity as derived from 10-min rainfall depth data for Ukkel (Brussels, Belgium): Implications for assessing soil erosion rates. J. Geophys. Res. Atmospheres 111. https://doi.org/10.1029/2006JD007169.
von Lützow, M., Kögel-Knabner, I., Ekschmitt, K., Flessa, H., Guggenberger, G., Matzner, E., Marschner, B., 2007. SOM fractionation methods: Relevance to functional pools and to stabilization mechanisms. Soil Biol. Biochem. 39, 2183–2207. https://doi.org/10.1016/j.soilbio.2007.03.007.
Wang, X., Jing, Z.-H., He, C., Liu, Q.-Y., Qi, J.-Y., Zhao, X., Xiao, X.-P., Zhang, H.-L., 2021. Temporal variation of SOC storage and crop yield and its relationship - A fourteen year field trial about tillage practices in a double paddy cropping system. China. Sci. Total Environ. 759, 143494 https://doi.org/10.1016/j.scitotenv.2020.143494.